ENERGY SAVING CONTROL STRATEGY OF BEAM PUMPING MOTOR SYSTEM BASED ON DOUBLE-FED INDUCTION MACHINES (DFIM)

Wei ZHAO[1], Wenle SONG[2], Guidong ZHU[3], Guangliang YANG[4], Shuchun CHEN[5]*

The efficiency of beam pumping motor system (BPMS) is influenced by complex mechanical movement and variable working conditions. Establishing appropriate energy saving strategies has been an important problem. A new minimum power root mean square (RMS) optimization control strategy based on double-fed induction machines (DFIM) is proposed in this paper. To validate the method, the simulation based on a CYJY10-4.2-53HB pumping unit is carried out. The results show that the input power of the BPMS can be reduced by 25.7% with the proposed strategy, which meets the practical application requirements.

Keywords: Beam pumping motor system; double-fed induction machine; energy saving; minimum power control

1. Introduction

Oil production industry is a typical high energy consumption industry in which beam pumping motor system (BPMS) is widely used due to its stable performance [1]. Because of complex load conditions of the BPMS, energy is transformed in many forms, such as electric energy, mechanical energy and kinetic energy [2]. This complex operation state leads to the low energy efficiency operation both on the power side and load side [3]. Therefore, the energy saving research of BPMS is necessary [4].

Nowadays, the energy-saving technology of BPMS includes variable frequency (VF) [5], intermittent supply control (ISC) [6] and linear motors [7] and so on. For example, in [8], an optimal feedback linearization control for permanent magnet machine is proposed which could admit non-constant reference torques. In [9], a new control method for BPMS is presented, which adopts rapid soft re-switching technology, and power saving ratio reaches 10%-25%. Most of methods mentioned above are uneconomic to replace old machines when they are

[1] S.E., State Grid Cangzhou Electric Supply Company, China, e-mail: 15103275643@126.com
[2] S.E., State Grid Cangzhou Electric Supply Company, China, e-mail: wlsong2009@163.com
[3] Eng., State Grid Cangzhou Electric Supply Company, China, e-mail: 1109748470@qq.com
[4] Master candidate, North China Electric Power University, China, e-mail: yang981010@163.com
[5] A.P., Hebei Software Institute, China, e-mail: hb_wangwz@163.com

still functioning [10]. Due to the increasing number of low production oil wells and effectiveness of VF control, this control method is widely used in the field [11]. The basic conception of this method is to regulate the frequency of power supply and the voltage is also changed accordingly [12]. In [13], a practical VF control strategy is proposed which controls the horsehead acceleration, increasing the efficiency during the up-stroke. However, traditional VF control assumes that speed reference of the motor remains constant, which limits the energy saving effect. However, few literatures apply VF control to the double-fed induction machine (DFIM) in the BPMS. In traditional speed tracking control of DFIM, the speed reference is set constant, which limits the energy saving effect because the speed is not automatically adjusted with the operation pf beam pumping unit.

This paper establishes the comprehensive mathematical model of pumping unit and DFIM. Based on the model, a new VF control method based on DFIM is proposed, in which speed reference of the control is determined through the optimization algorithm, making the objective function of output active power reach the minimum. Additionally, the simulation results of different Fourier expansion times and average motor speed are compared. The recommended application scenario of the motor is given to obtain better energy saving effect. Finally, the proposed optimization control method is verified through a CYJY10-4.2-53HB beam pumping unit. The results show that the pumping unit power is reduced by 25.7% compared with the traditional method, which verifies the effectiveness and practicability of the strategy. The research results of this paper provide new energy saving approach for oil product industry in oil field.

2. Mathematical model of BPMS

2.1 Mathematical model of pumping unit

The BPMS is mainly composed of motor, four-bar linkage, balancing device, which is shown in Fig. 1. The torque acts on the crank shaft through the belt and gear box, and drives the horsehead to move back and forth between the upper and lower dead points through four-bar linkage.

Fig. 1. Pumping unit

For the convenience of research, the following assumptions are made:

1) Grid voltage and frequency are constant;

2) The deformation of the transmission parts from the rotor shaft to the suspension point of the pumping unit is ignored.

3) The resistance force of the pump is not considered;

4) The oil-water mixture is in the wellbore. The dynamic viscosity and the well fluid temperature are constant.

The rotating motion of the crank shaft is transformed into linear motion of the horsehead. The working diagram is shown in Fig.2.

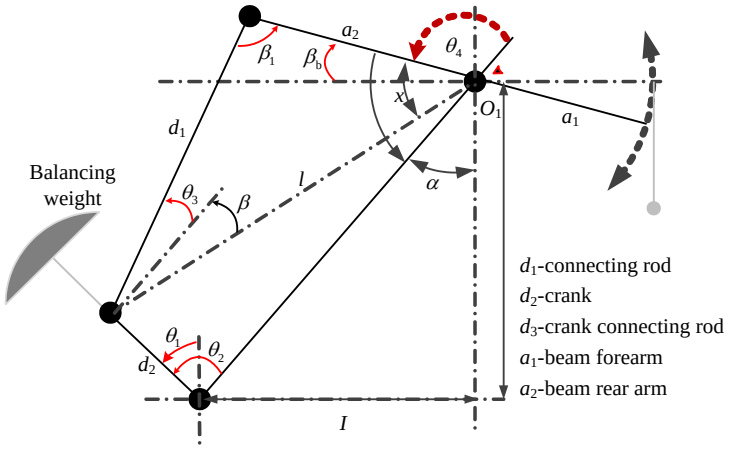

Fig. 2. Schematic diagram of crank movement

The equation of crank motion is shown in (1).

$$J_e\ddot{\theta}_1 + \frac{1}{2}\dot{\theta}_1 \frac{dJ_e}{d\theta_1} = M_{ed} - M_{ef} \tag{1}$$

where J_e is the equivalent moment of inertia of the BPMS; M_{ed} represents the equivalent driving torque of crankshaft; M_{ef} represents the equivalent resistance moment of crankshaft.

The operation cycle of pumping units is generally 6-10 seconds, while the operation cycle of low production wells is usually more than 10 seconds, and the crank shaft speed is one tenth of the motor speed. Therefore, it can be assumed that the crank shaft speed is unchanged. The crank rotation angle is θ_1 can be obtained as follows:

$$\theta_1 = \theta_0 + \int_{t_0}^{t_1} \omega_r dt \tag{2}$$

where θ_0 represents the initial angle of crankshaft, ω_r represents the electric angular speed.

The equivalent resistance torque includes horsehead load and balance load, as shown in (3) and (4). The loss from motor shaft to crank shaft is obtained by (5). When P_{2q} is negative, the system is in power generation condition.

$$M_{ed} = \eta H_{DQ} T_2 \tag{3}$$

$$M_{ef} = T_F \left(P_{RL} - B_w\right) H_{CL} - M_m \sin\left(\theta_1 - \tau\right) \tag{4}$$

$$P_{2q} = P_2 - M_{ed}\Omega_r \tag{5}$$

where H_{DQ} represents the efficiency from motor to crank; T_2 is the motor output torque; η is the transmission ratio from motor shaft to crank shaft; T_F is the torque factor of pumping unit; P_{RL} is the horsehead suspension point load of the pumping unit; B_W is the unbalanced weight; H_{CL} indicates the efficiency from the suspension point to crank; M_m represents the maximum value of balancing device torque; τ is the lag angle. p_{2q} is the energy loss from motor shaft to crank shaft; Ω_r represents the mechanical angular speed; P_2 is the output power.

2.2 Mathematical model of DFIM

The model of DFIM includes finite element model and steady-state T-type equivalent circuit model [14-16]. Although the finite element model has accurate calculation results, it cannot meet the requirement of real time in field application. Therefore, the steady-state T-type circuit model of DFIM is adopted, which

includes voltage equation, flux linkage equation and rotor motion equation. For the convenience of analysis, iron loss is ignored.

The voltage equation is shown in (6):

$$\begin{cases} U_{ds} = R_s I_{ds} - \omega_B \left(L_{ss} I_{qs} + L_m I_{qr} \right) \\ U_{qs} = R_s I_{qs} + \omega_B \left(L_{ss} I_{ds} + L_m I_{dr} \right) \\ U_{dr} = R_r I_{dr} - \left(\omega_B - \omega_r \right) \left(L_{rr} I_{qr} + L_m I_{qs} \right) \\ U_{qr} = R_r I_{qr} + \left(\omega_B - \omega_r \right) \left(L_{rr} I_{dr} + L_m I_{ds} \right) \end{cases} \tag{6}$$

The rotor motion equation is shown in (7):

$$p\omega_r = \frac{P\left(T_e - T_L\right)}{J} \tag{7}$$

The electromagnetic torque is shown in (8):

$$T_e = PL_m \left(I_{qs} I_{dr} - I_{ds} I_{qr} \right) \tag{8}$$

The rotor side power is shown in (9):

$$P_2 = m\left[I_r^2 R_r + s\left(P_1 + I_s^2 R_s \right) \right] \tag{9}$$

where U_{ds}, U_{qs}, U_{dr}, U_{qr} are the stator and rotor voltage in dq coordinate; I_{ds}, I_{qs}, I_{dr} and I_{qr} are the stator and rotor current in dq coordinate; ω_B is synchronous electrical angular velocity; L_{ss}, L_{rr} and L_m are stator and rotor total leakage inductance and magnetizing inductance respectively; R_s and R_r are stator and rotor resistance; p is the differential operator; J is the moment of inertia; P is the pole pair number; T_e and T_L are electromagnetic torque and load torque.

The power flow diagram of DFIM is shown in Fig. 3:

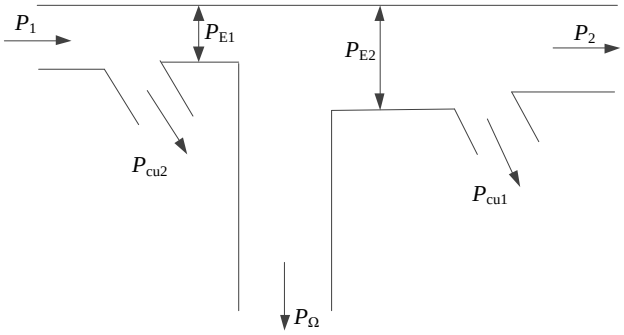

Fig. 3. Power flow of DFIM

Through the speed tracking control of the DFIM, the motor speed $n(t)$ will change periodically with the operation of the pumping unit according to the speed reference $n_{ref}(t)$. Therefore, the motor speed can be expanded according to Fourier series, as shown in (10).

$$n = a_0 + \sum_{m=1}^{M}\left[a_{\mathrm{n}}\cos\left(\frac{2\pi mt}{T_0}\right) + b_n\cos\left(\frac{2\pi mt}{T_0}\right)\right] \tag{10}$$

where a_{n} and b_{n} are the coefficients of Fourier series; M is the Fourier expansion number.

Output torque T_2 can be obtained as follows:

$$T_2 = T_e - T_{\mathrm{m}} - T_{\mathrm{a}} \tag{11}$$

where T_{a} is the additional loss torque; T_{m} is the mechanical loss torque.

The coupling equation of pumping unit torque and motor output torque can be obtained by (3) and (11), as shown in (12).

$$M_{\mathrm{ed}} = \eta H_{\mathrm{DQ}}\left[PL_{\mathrm{m}}\left(I_{\mathrm{qs}}I_{\mathrm{dr}} - I_{\mathrm{ds}}I_{\mathrm{qr}}\right) - T_{\mathrm{m}} - T_{\mathrm{a}}\right] \tag{12}$$

3. Energy saving strategy of DFIM

3.1 Objective function

For the BPMS with variable frequency controlled DFIM, after expanding the speed reference $n_{\mathrm{ref}}(t)$ into Fourier series, the output power $P_2(t)$ of DFIM can be obtained from the motor torque and speed, as shown in (13).

$$P_2(t) = \frac{\pi M_{\mathrm{ed}} n_{\mathrm{ref}}(t, a_0, a_1, b_1, \cdots, a_n, b_n)}{30\eta H_{\mathrm{DQ}}} \tag{13}$$

In order to achieve the purpose of energy saving, the RMS of output power is taken as the objective function, as shown in (14). The integral in the formula is converted into the sum of discrete points, as shown in (15), to simplify the calculation.

$$\min P_e\left(a_0, a_1, b_1, \cdots, a_{\mathrm{n}}, b_{\mathrm{n}}\right) = \sqrt{\frac{1}{2\pi}\int_0^{2\pi} P_2^2 \mathrm{d}\theta} \tag{14}$$

$$\frac{1}{2\pi}\int_0^{2\pi} P_2^2 \mathrm{d}\theta = \frac{\sum_{k=1}^{K} P_2^2}{K} \tag{15}$$

where K means that the integral is converted into the sum of K discrete points. It is assumed that k=50 in this paper.

3.2 Constraint condition

1) Impulse constraint

The pumping unit sprint remains unchanged before and after frequency conversion, as follows:

$$n_{\mathrm{f}} - n_{\mathrm{set}} = 0 \tag{16}$$

where n_{f} is the pumping unit stroke times after variable frequency control; n_{set} is the set value of impulse times.

2) Average speed constraint

For sake of the operation of the motor, average speed in a cycle can be set as kn_1, as shown in (17).

$$\int_0^T n_{\text{ref}}\,\mathrm{d}t = kn_1 \tag{17}$$

where k is the speed coefficient, which is given by the specific operating conditions of the pumping unit; n_1 is the synchronous speed.

3) Speed range constraint

The speed regulation range of the DFIM is generally above $0.6n_1$. Besides, considering the mechanical loss and operation safety of the pumping unit, the speed cannot be too high, so the speed regulation constraints are as follows:

$$0.6n_1 \le n(t) \le n_1 \tag{18}$$

3.3 Mathematical model and optimization algorithm

The mathematical mode for optimizing speed reference of the DFIM can be obtained in (19), in which the RMS of the pumping unit output power is minimized.

$$\left.\begin{array}{c} F(x) = \min P_{\text{e}}(a_0, a_1, b_1, \cdots, a_n, b_n) \\ n_{\text{f}} = n_{\text{set}} \\ 0.6n_1 \le n(t) \le n_1 \\ \int_0^T n_{\text{ref}}\,\mathrm{d}t = kn_1 \end{array}\right\} \tag{19}$$

The model includes objective function and three constraints: impulse constraint, average speed constraint and speed range constraint. Where the objective function $F(x)$ is the RMS of the output power of the pumping unit, which is a function of the Fourier coefficient.

In this paper, the interior point method is used to solve the above model. Its basic idea is to convert the constrained optimization problem to an unconstrained problem, and then update utility function by the optimization iteration process to make the algorithm converge. The algorithm is suitable for linear programming and nonlinear convex optimization problems.

4. Optimization design and evaluation of simulation

4.1 Simulation settings

Fig. 4 shows the established model of BPMS based on DFIM. The model includes the following 4 parts: 1) Speed reference generator. 2) VF control in the rotor side. 3) VF control in the grid side. 4) Primary circuit. It is worth mentioning that according to Fourier decomposition, the sum of several sinusoidal signals constitutes the speed reference value of the motor. The main parameters are as

follows: The pumping depth of the oil field is 900m; The type of the pumping unit is CYJY10-4.2-53HB, the stroke of the suspension point is 6 times /min, the crankshaft moment of inertia is 3025 kg·m^2, and the stroke is 2.9973m; The stator resistance of DFIM is 0.0026 Ω, the rotor resistance is 0.0029 Ω, the stator and rotor leakage inductance is 0.000087H. Specific parameters are shown in Table 1. Fig. 5 shows the simulated torque of the pumping unit.

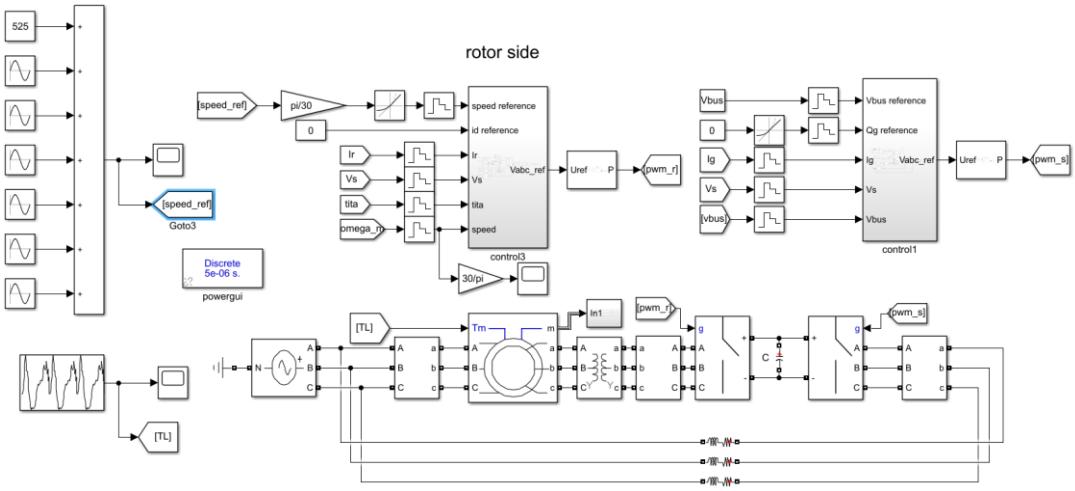

Fig. 4. Model of DFIM with beam pumping unit

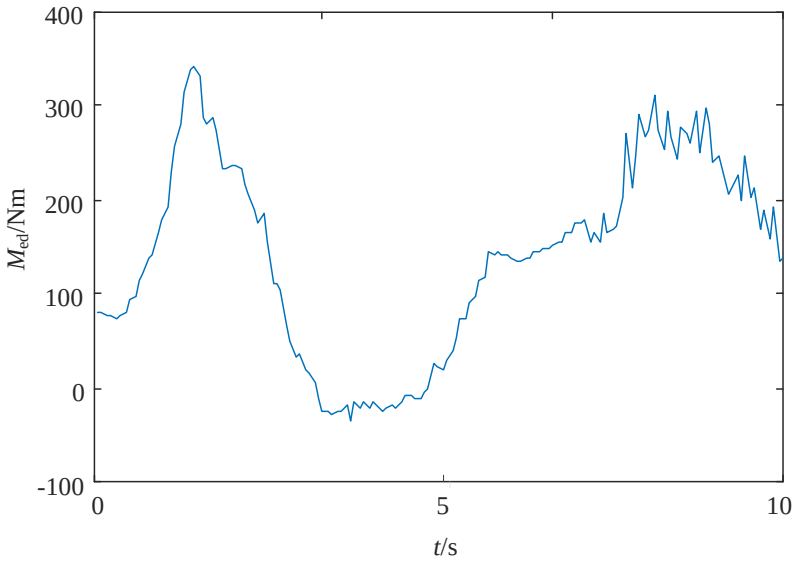

Fig. 5. Output torque of pumping unit

Table 1

Main parameters of simulation

Equipment	Parameter	Value
Oil well	Pump depth /m	900
	Liquid height /m	700
	Clearance between plunger and barrel /m	0.2
	Hydrodynamic viscosity /(Pa·s)	0.1
Beam pumping unit	Type	CYJY10-4.2-53HB
	Suspension stroke times /(time/min)	6
	Crank moment of inertia /(kg·m^2)	3025
	Crank radius /m	0.81
	stroke /m	2.9973
	Connecting rod length /m	3.6
	Beam forearm /m	4.4
	Beam rear arm /m	2.5

The simulated torque data is substituted into (13), and the coefficients a_n and b_n of the Fourier expansion of the speed reference $n_{ref}(t)$ of the DFIM can be obtained by (19) using internal point optimization algorithm. In order to compare the results of different expansion times of $n_{ref}(t)$, n=1, 2 and 3 are calculated respectively. In addition, in order to compare the optimization results of pumping units under different working conditions, the speed coefficients k=0.7 and 0.75 are analyzed.

4.2 Analysis of simulation results

The optimization results are shown in Table 2, and the curve of $n_{ref}(t)$ is shown in Fig. 6.

Table 2

Minimum average power optimization results

k	n	P_e/W	a_0	a_1	b_1	a_2	b_2	a_3	b_3
0.7	1	8873	525	-68	32	—	—	—	—
	2	8472	525	-97	38	32	-31	—	—
	3	8274	525	-96	70	26	-67	10	25
0.75	1	9294	563	-102	48	—	—	—	—
	2	8870	563	-136	64	24	-29	—	—
	3	8755	563	-130	53	36	-42	17	-5

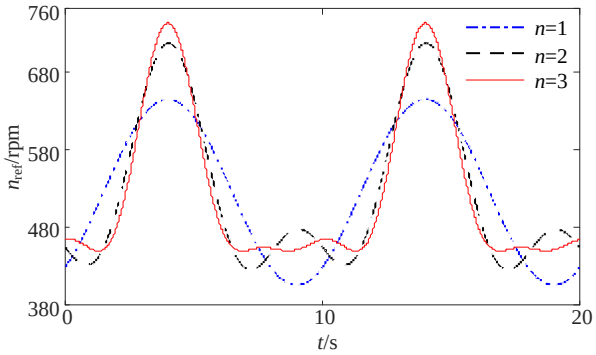

(a) k=0.7

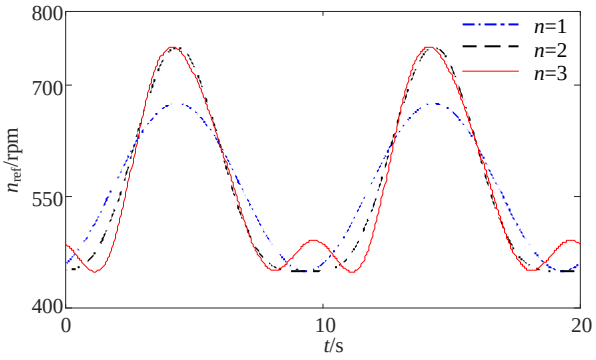

(b) k=0.75

Fig. 6. Speed reference

It can be seen from Table 2 that, with the increase of n, the speed reference of DFIM is more accurate. Meanwhile, the average active power P_e is smaller, indicating that the energy consumption is reduced. When n>3, with the increase of n, the improvement of energy saving effect is not obvious. In order to simplify calculation, the case of n>4 is no longer calculated.

The speed of the proposed and traditional control methods is compared in Fig. 7. When the traditional speed tracking control is adopted, the speed remains unchanged after rising to a constant value, which cannot change periodically with the operation of the beam pumping unit, resulting in huge power consumption. When using the proposed control method, the speed reference changes with the torque of beam pumping motor. When k=0.7, the speed changes in the range of 450~743rpm. When k=0.75, the speed changes in the range of 450~752rpm. In an operation cycle, when the output torque is low, the speed reference value is high and vice versa. The reason is that the power is equal to the product of torque and mechanical angular velocity, so the fluctuation of the power is relatively small in one operation cycle, which verifies the effectiveness of proposed control method.

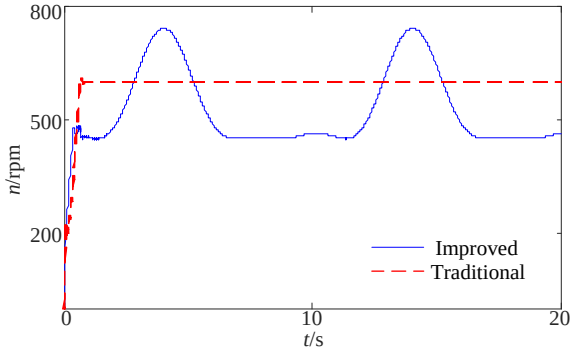

(a) k=0.7

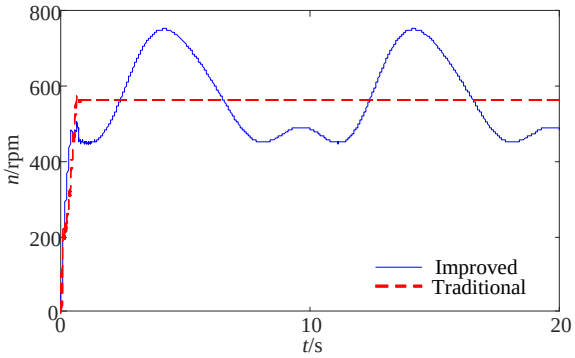

(b) k=0.75

Fig. 7 Speed curve of DFIM

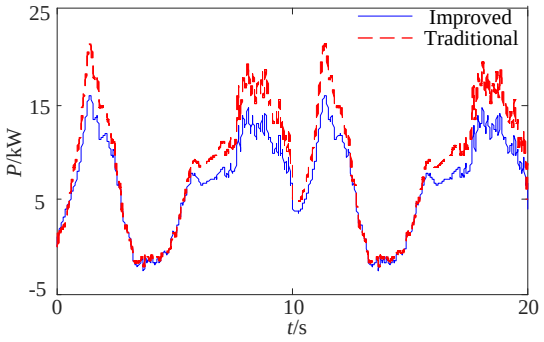

(a) k=0.7

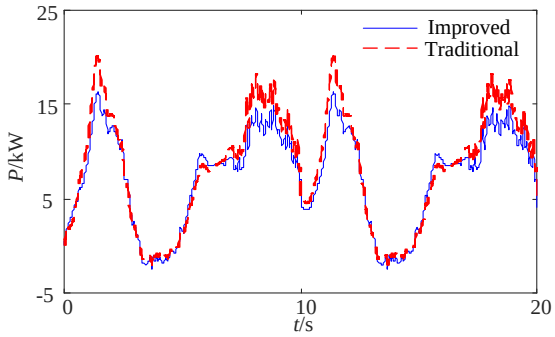

(b) k=0.75

Fig. 8 Pumping unit power

The consumed power with different control methods is shown in Fig. 8. When the instantaneous power of the traditional strategy is high, the instantaneous power of the optimization strategy decreases significantly, indicating that the optimization method reduces power fluctuations effectively, and this effect is more significant at peak power. Besides, when k is smaller, the motor speed is lower, resulting in smaller RMS motor power. When k=0.7, the output power of the beam pumping machine is reduced by 25.7% compared with the traditional control strategy, which verifies the validity of the optimal control strategy. When k=0.75, the output power is only reduced by 21.4% compared with the traditional control strategy, which indicates that the represented control strategy proposed is more suitable for the condition that motors are operating at a relatively lower speed (k=0.7).

5. Economic Benefit Analysis

Taking a 37kW BPMS as an example, the cost of traditional high-capacity frequency converter control and proposed DFIM control are compared in Table 3.

Table 3

Cost comparison of different control methods

Control method	Traditional frequency converter control		DFIM control	
Item	Equipment	Cost (CNY)	Equipment	Cost (CNY)
1	37kW induction motor	4200	37kW DFIM	5200
2	37kW four quadrant frequency converter	18500	15kW four quadrant frequency converter	9000
Total cost (CNY)	22700		14200	

Under the same conditions, the cost of proposed DFIM control is lower than that of traditional frequency converter control. Even if the traditional frequency converter control only introduces 37kW frequency converters without replacing the induction motor, it still costs 18500 CNY, which is higher than total cost of DFIM control (14200 CNY). This is because the capacity of frequency

converter of DFIM control is smaller (15kW). Therefore, the proposed DFIM control is more economical and is worthy of real application.

6. Conclusions

Aiming at the energy saving problem of high energy consumption beam pumping units, this paper puts forward a new minimum power optimization strategy based on DFIM. The speed reference of the DFIM is expanded by Fourier series, and the Fourier coefficient is determined by interior point method to minimize the power of beam pumping units. Compared with the traditional method, the consumed power is reduced by 25.7%.

The proposed control method is useful when motor speed is relatively low, while the energy saving effect will be weakened when the speed is high. Therefore, it is suggested to apply this control strategy to motors operating with relative high speed.

An energy saving method based on DFIM is presented, which needs to obtain the operating characteristics of pumping units. However, more intelligent energy-saving technology under complex conditions such as grid fluctuations needs further research.

Acknowledgement

This work was supported by Technology Project of State Grid Cangzhou Electric Supply Company under Grant No. KJ2021-009.

R E F E R E N C E S

[1]. *H. Zhao, Y. Wang, Y. Zhan, G. Xu and X. Cui*, "Rapid Soft Re-switching Strategy of Intermittent Supply for Energy Saving in Beam Pumping Motors Systems with Dynamic Load Conditions", in IEEE Trans. Ind. Appl., **vol. 55**, no. 4, July-Aug. 2019, pp. 3343-3353.

[2]. *H. Zhao, Y. Wang, Y. Zhan, G. Xu, X. Cui, and J. Wang*, "Practical Model for Energy Consumption Analysis of Beam Pumping Motor Systems and Its Energy-Saving Applications", in IEEE Trans. Ind. Appl., **vol. 54**, no. 2, Mar.-Apr. 2018, pp. 1006–1016.

[3]. *S. G. Gibbs and D. L. Miller*, "Inferring Power Consumption and Electrical Performance From Motor Speed in Oil-Well Pumping Units", in IEEE Trans. Ind. Appl., **vol. 33**, no. 1, Jan.-Feb. 1997, pp. 187-193.

[4]. *X. Li, K. Tian, C. Li, Y. Zhou, L. Li and J. Hong*, "Linear Electromagnetic Oil Pumping Unit Based on the Principle of Coil Gun", in IEEE Trans. Magn., **vol. 45**, no. 1, Jan. 2009, pp. 347-350.

[5]. *H. Zhao, B. Wang, Y. Wang, and H. Li*, "Research on Sectionalized Energy-Saving Control Strategy Based on Frequency and Voltage Regulator Technique for Induction Motor With Potential Loads", in Proc. CSEE. **vol. 35**, no 06, Mar. 2015, pp. 1490-1497.

[6]. *X. Cui, Y. Luo, Y. Yang, Y. GUO, H. Wang, and X. Liu*, "Energy Saving Theory and Approach for Asynchronous Motor Under the Periodically Variable Running Condition", in Proc. CSEE. **vol. 28**, no 18, Jun. 2008, pp. 90-97.

[7]. *L. Li, S. Cui, P. Zheng, X. Guo, S. Cheng and Y. Wang*, "Experimental Study on a Novel Linear Electromagnetic Pumping Unit", in IEEE Trans. Magn., Jan. 2001, **vol. 37**, no. 1, pp. 219-222.

[8]. *S. Mallik, K. Mallik, A. Barman, and D. Maiti*, "Efficiency and Cost Optimized Design of an Induction Motor Using Genetic Algorithm", in IEEE Trans. Ind. Electron., **vol. 64**, no. 12, Dec. 2017, pp. 9854-9863.

[9]. *Y. L. Luo, X. S. Cui, H. S. Zhao, Y. L Wang, Y. Luo, and D. Q. Zhang*, "A Multifunction Energy-Saving Device With a Novel Power-Off Control Strategy for Beam Pumping Motors", in IEEE Trans. Ind. Appl., **vol. 47**, no. 4, Jul.-Aug. 2011, pp. 1605–1611,

[10]. *J. Lu, J. He, C. Mao, W. Wu, D. Wang and W. -J. Lee*, "Design and Implementation of a Dual PWM Frequency Converter Used in Beam Pumping Unit for Energy Saving", in IEEE Trans. Ind. Appl., **vol. 50**, no. 5, Sept.-Oct. 2014, pp. 2948-2956.

[11]. *R. Azizipanah-Abarghooee and M. Malekpour*, "Smart Induction Motor Variable Frequency Drives for Primary Frequency Regulation", in IEEE Trans. Energy Convers., **vol. 35**, no. 1, Mar. 2020, pp. 1-10.

[12]. *S. V. Giannoutsos and S. N. Manias*, "A Systematic Power-Quality Assessment and Harmonic Filter Design Methodology for Variable-Frequency Drive Application in Marine Vessels", in IEEE Trans. Ind. Appl., **vol. 51**, no. 2, March-April 2015, pp. 1909-1919.

[13]. *Y. Wang, H. H. Eldeeb, H. Zhao and O. A. Mohammed*, "Sectional Variable Frequency and Voltage Regulation Control Strategy for Energy Saving in Beam Pumping Motor Systems", in IEEE Access, **vol. 7**, Jul. 2019, pp. 92456-92464.

[14]. *V. S. S. Kumar and D. Thukaram*, "Alternate Proof for Steady-State Equivalent Circuit of a Doubly Fed Induction Machine", in IEEE Trans. Power Electron., **vol. 31**, no. 8, Aug. 2016, pp. 5378-5383.

[15]. *J. Ge, W. Xu, Y. Liu and F. Xiong*, "Novel Equivalent Circuit Model Applicable to All Operation Modes for Brushless Doubly Fed Induction Machines", IEEE Trans. Ind. Electron., **vol. 69**, no. 12, Dec. 2022, pp. 12540-12550.

[16]. *D. Kim and B. Kwon*, "A Novel Equivalent Circuit Model of Linear Induction Motor Based on Finite Element Analysis and Its Coupling With External Circuits", in IEEE Trans. Magn., **vol. 42**, no. 10, Oct. 2006, pp. 3407-3409.